AGU PUBLICATIONS

Global Biogeochemical Cycles

RESEARCH ARTICLE
10.1002/2014GB005014

Key Points:
- Biotic iron pools are of similar magnitude in low- and high-iron waters
- Iron quotas and *fe* ratios together primarily set the size of biotic iron pools
- Iron-rich microbes dominate biotic pools and iron recycling in HNLC waters

Supporting Information:
- Readme
- Table S1

Correspondence to:
P. W. Boyd,
Philip.Boyd@utas.edu.au

Citation:
Boyd, P. W., R. F. Strzepek, M. J. Ellwood, D. A. Hutchins, S. D. Nodder, B. S. Twining, and S. W. Wilhelm (2015), Why are biotic iron pools uniform across high- and low-iron pelagic ecosystems?, *Global Biogeochem. Cycles*, *29*, 1028–1043, doi:10.1002/2014GB005014.

Received 13 OCT 2014
Accepted 15 JUN 2015
Accepted article online 17 JUN 2015
Published online 24 JUL 2015

Why are biotic iron pools uniform across high- and low-iron pelagic ecosystems?

P. W. Boyd[1,2], R. F. Strzepek[3,4], M. J. Ellwood[5], D. A. Hutchins[6], S. D. Nodder[7], B. S. Twining[8], and S. W. Wilhelm[9]

[1]NIWA Centre for Chemical and Physical Oceanography, Department of Chemistry, University of Otago, Dunedin, New Zealand, [2]Now at Institute for Marine and Antarctic Studies, University of Tasmania, Hobart, Tasmania, Australia, [3]Department of Chemistry, University of Otago, Dunedin, New Zealand, [4]Now at Research School of Earth Sciences, Australian National University, Canberra, Australia, [5]Research School of Earth Sciences, Australian National University, Canberra, Australia, [6]Marine and Environmental Biology, Department of Biological Sciences, University of Southern California, Los Angeles, California, USA, [7]National Institute of Water and Atmospheric Research (NIWA), Wellington, New Zealand, [8]Bigelow Laboratory for Ocean Sciences, East Boothbay, Maine, USA, [9]Department of Microbiology, University of Tennessee, Knoxville, Tennessee, USA

Abstract Dissolved iron supply is pivotal in setting global phytoplankton productivity and pelagic ecosystem structure. However, most studies of the role of iron have focussed on carbon biogeochemistry within pelagic ecosystems, with less effort to quantify the iron biogeochemical cycle. Here we compare mixed-layer biotic iron inventories from a low-iron (~0.06 nmol L^{-1}) subantarctic (FeCycle study) and a seasonally high-iron (~0.6 nmol L^{-1}) subtropical (FeCycle II study) site. Both studies were quasi-Lagrangian, and had multi-day occupation, common sampling protocols, and indirect estimates of biotic iron (from a limited range of available published biovolume/carbon/iron quotas). Biotic iron pools were comparable (~100 ± 30 pmol L^{-1}) for low- and high-iron waters, despite a tenfold difference in dissolved iron concentrations. Consistency in biotic iron inventories (~80 ± 24 pmol L^{-1}, largely estimated using a limited range of available quotas) was also conspicuous for three Southern Ocean polar sites. Insights into the extent to which uniformity in biotic iron inventories was driven by the need to apply common iron quotas obtained from laboratory cultures were provided from FeCycle II. The observed twofold to threefold range of iron quotas during the evolution of FeCycle II subtropical bloom was much less than reported from laboratory monocultures. Furthermore, the iron recycling efficiency varied by fourfold during FeCycle II, increasing as stocks of new iron were depleted, suggesting that quotas and iron recycling efficiencies together set biotic iron pools. Hence, site-specific differences in iron recycling efficiencies (which provide 20–50% and 90% of total iron supply in high- and low-iron waters, respectively) help offset the differences in new iron inputs between low- and high-iron sites. Future parameterization of iron in biogeochemical models must focus on the drivers of biotic iron inventories, including the differing iron requirements of the resident biota, and the subsequent fate (retention/export/recycling) of the biotic iron.

1. Introduction

Over the last two decades the supply of iron has been shown to exert a major influence on the biogeochemical cycles of many elements, such as Nitrogen, Carbon, Silicon, and Sulfur, in both high and low latitude oceanic waters [*Hutchins and Bruland*, 1998; *Turner et al.*, 2004; *Boyd et al.*, 2007; *Moore and Doney*, 2007]. Biogeochemical modeling studies predict that iron supply limits the growth rates of diatoms, small phytoplankton, and nitrogen fixers across 28%, 36%, and 44% of the global ocean, respectively [*Moore et al.*, 2004]. At low latitudes, elevated iron supply often stimulates the growth of nitrogen fixers in oligotrophic waters with excess phosphate [*Moore et al.*, 2009]. At high latitudes, increased iron supply, from natural [*Blain et al.*, 2007] and purposeful [*Boyd et al.*, 2007] enrichment, increases rates of primary production and often shifts the phytoplankton community toward one dominated by large diatoms [*Martin et al.*, 1989].

The central aims of mesoscale in situ iron enrichments and regional studies of naturally high-iron waters have been to determine the extent that exogenous iron supply drives primary productivity, and the subsequent downward export of algal carbon [*Boyd et al.*, 2007]. Thus, the main focus of most previous studies has

been on determining the ratio of iron supplied to carbon fixed and subsequently exported [*de Baar et al.*, 2008]. This emphasis on better understanding the ocean's carbon biogeochemistry has resulted in the iron biogeochemical cycle receiving less attention [*Boyd and Ellwood*, 2010].

The central role that biological uptake plays in driving biogeochemical cycles of trace metals in the ocean has been recognized within the GEOTRACES science plan (http://www.geotraces.org/science/science-plan#), where it forms a key component of theme two on the internal cycling of trace elements. Prior to GEOTRACES, there have been a limited number of studies investigating the relationship between the magnitude of iron supply, the consequent partitioning into biotic iron pools, and biological iron recycling [*Bowie et al.*, 2001; *Frew et al.*, 2006; *Strzepek et al.*, 2005]. Although it is now possible to more readily measure the iron content of individual cells [see *Twining and Baines*, 2013], previous studies had to quantify the magnitude of biotic iron, within the pelagic food web, indirectly. Studies such as *Sarthou et al.* [2008] in the high-iron Southern Ocean or *Bowie et al.* [2009] in low-iron subantarctic waters employed biovolume/carbon algorithms, in conjunction with abundance data, to compute biotic carbon stocks and converted them to biotic iron using published iron quotas.

Boyd and Ellwood [2010], in a review of the oceanic iron biogeochemical cycle, made the first detailed intercomparison of the partitioning of biotic iron pools across pelagic food webs using examples from high-iron [Kerguelen Ocean and Plateau compared Study (KEOPS, 51°S 73°E)] [*Sarthou et al.*, 2008] versus low-iron, high nitrate-low chlorophyll (HNLC) waters (FeCycle, 46°S 179°E) [*Boyd et al.*, 2005]. *Boyd and Ellwood* [2010] revealed that the magnitude of biotic iron pools was similar between the high-iron waters at the KEOPS site and the low-iron FeCycle study site, but that community composition differed between sites (for example, diatoms vs. prokaryotic cyanobacteria), and hence, different combinations of plankton-specific iron quotas were used at each site to estimate the magnitude of biotic iron pools.

Here we investigate whether the trend in *Boyd and Ellwood* [2010]—that biotic iron pools are comparable across high- and low-iron pelagic ecosystems—holds for other high- and low-iron pelagic systems (ranging from Southern Ocean polar to subtropical seasonally oligotrophic waters) that were studied using quasi-Lagrangian, multi-day occupations. We also explore to what extent the apparent uniformity across biotic iron pools is driven by artifacts (use of the same published iron quotas), the different iron quotas of the resident biota that characterize each ecosystem, and/or other facets of regional iron biogeochemical cycles. Specifically, the intercomparison between the low-iron FeCycle and high-iron FeCycle II study enables a detailed assessment of the relative role of biological iron recycling in determining the fate of biotic iron at these contrasting sites which represent end-members for open ocean regions. Our investigation provides valuable insights into the main biological drivers of pelagic iron biogeochemistry across polar to subtropical oceanic provinces.

2. Characteristics of Low- and High-Iron Sites

Both studies took place east of New Zealand. FeCycle was conducted in Austral summer (February 2003) in low-iron, HNLC subantarctic waters (46°S 179°E), and FeCycle II took place in high-iron, low macro-nutrient subtropical waters (39°S 178°W) in Austral spring (September/October 2008). The FeCycle site is representative of the "sub-Antarctic water ring" that comprises ~40% of the open Southern Ocean [*Banse*, 1996], and the FeCycle II site is typical of the seasonally oligotrophic subtropical biome [*Longhurst*, 2007]. FeCycle used the tracer sulfur hexafluoride (SF_6) to chemically label a patch of ~100 km^2 of HNLC surface waters to provide a 10 day quasi-Lagrangian sampling opportunity. FeCycle II was located in a quiescent eddy center and was also sampled in a quasi-Lagrangian manner for 12 days, but without SF_6 addition. Detailed background oceanographic information/ancillary measurements are presented in *Boyd et al.* [2005] and *Boyd et al.* [2012] for FeCycle and FeCycle II, respectively. Both studies were characterized by identical methods, and in most cases, analyses were done by the same participants on each voyage. One major distinction between these studies is that the HNLC waters during FeCycle were in steady state, as evidenced for example in the dissolved and particulate iron inventories [*Croot et al.*, 2007] and microbial food-web structure [*Strzepek et al.*, 2005]. FeCycle II was a GEOTRACES process study of the dynamic evolution and decline of the spring bloom, and thus sampled a system that was inherently not at steady state [*Boyd et al.*, 2012; *Ellwood et al.*, 2014].

At the low-iron FeCycle site, dissolved iron (DFe) was ~60 pmol L^{-1}, and the supply of new iron was dominated by atmospheric deposition [*Boyd et al.*, 2005]. In contrast, at the high-iron FeCycle II site, supply was driven by

Table 1. Summary of the Community Composition of Microbes, Phytoplankton, and Grazers Across the Five Study Sites Featured[a]

Site	Characteristics	Cyanobacteria	Auto-flags	Diatoms	Microzoo	Mesozoo
FeCycle[b]	Subantarctic HNLC	Prokaryotic (*Synecho.*)	Mixed comm. (low abundances)	Low abundances, mixed comm.	Mixed comm.	Calanoid and neocalanoid copepods
FeCycle II[c]	Subtropical high iron	Prokaryotic (*Synecho.*)	Mixed comm. (low abundances)	*Asterionellopis* bloom	Mixed comm.	Mainly calanoid copepods
SOIREE HNLC[d]	Polar HNLC	Eukaryotic	Mixed comm. (low abundances)	Low abundances, mixed comm.	Mixed comm.	Mainly calanoid copepods
SOIREE high iron[d]	Polar high iron	Eukaryotic	Mixed comm. (high abundances)	*Fragiliariopsis* bloom	Mixed comm.	Mainly calanoid copepods
KEOPS[e]	Island wake high iron	Pro and Euk's (low abundances)	Mixed comm. (low abundances)	*Chaetoceros* bloom	Mixed comm.	Mixed community (including euphausiids)

[a]Heterotrophic bacteria were present at all sites, but there is insufficient data resolution to distinguish any site-specific differences in bacterial community structure. Different community structures for mesozooplankton make it problematic to apply site-specific Fe quotas (for example, from FeCycle II) to other locales. Auto-flags, microzoo, and mesozoo denote autotrophic nanoflagellates, microzooplankton, and mesozooplankton. Comm., Synecho., Pro., and Euk. denote Community, *Synechococcus*, Prokaryote, and Eukaryote, respectively.
[b]*Strzepek et al.* [2005].
[c]*Boyd et al.* [2012]; *Twining et al.* [2014].
[d]*Bowie et al.* [2001] and references therein.
[e]*Sarthou et al.* [2008] and references therein.

lateral transport of iron derived from continental margin environments prior to eddy formation, resulting in an early spring DFe of ~0.6 nmol L^{-1}, which declined to 0.1 nmol L^{-1} during the bloom [*Boyd et al.*, 2012; *Ellwood et al.*, 2014]. A return voyage near the FeCycle II site (September 2012) also revealed an early season "reserve" DFe of ~0.5 nmol L^{-1} (P. W. Boyd, unpublished data). Different pelagic biota characterized these sites (Table 1), with a microbial food web comprising pico- and nanoplankton at FeCycle [*Strzepek et al.*, 2005], and a diatom-dominated spring bloom with high mesozooplankton stocks evident during FeCycle II [*Boyd et al.*, 2012]. This larger-celled FeCycle II community was succeeded by a microbially dominated food web as the diatom bloom declined [*Boyd et al.*, 2012; *Matteson et al.*, 2012].

2.1. Methods and Materials

The methods used to obtain all data shown in Figures 1, 3, and 5 are presented in Tables 2 and 3. Protocols reported in *Boyd et al.* [2005] and *Boyd et al.* [2012] were used to derive the data presented in Figure 2. The methods used to obtain the downward particulate iron fluxes using free-drifting surface-tethered sediment traps are reported in *Frew et al.* [2006] and *Boyd et al.* [2012]. The data presented on the range of phytoplankton iron quotas, from published laboratory culture and field studies in Table S1 of the supporting information, were compiled from the literature.

As is evident from Table 2, there are a limited number of biovolume to carbon biomass conversion factors available for open ocean microbes, phytoplankton, and zooplankton. Most of these estimates for microbes and phytoplankton were obtained from lab-culture studies, such as *Verity et al.* [1992] who used >10 representative species to derive the biovolume to C algorithms. The zooplankton carbon algorithms were mainly obtained from collations of data sets from a wide range of net-caught zooplankton [*Mauchline*, 1998]. These algorithms have been subjected to robust appraisals [*Montagnes et al.*, 1994] where their validity across a wide range of lab-cultured species has been confirmed. Hence, the algorithms have been used with confidence in pelagic marine carbon budgets such as *Fasham et al.* [1999].

Calculations of total biotic iron have relied upon a combination of taxon-specific published Fe quotas (such as heterotrophic bacteria) and site-specific direct measurements of taxon-specific quotas [for example, diatoms and eukaryotic cyanobacteria at the Southern Ocean Iron Release Experiment (SOIREE) site (61°S 140°E) by *Bowie et al.*, 2009]. However, as for carbon/biovolume algorithms, an equally small range of published Fe quotas has been applied to calculations of biotic iron pools for microbes, phytoplankton, and mesozooplankton (Table 3). The narrow range of published Fe quotas used reflects the difficulties in making these measurements and hence a tendency to employ the selected quotas used in earlier studies. For example, *Sarthou et al.* [2008] based their biotic iron budget on prior efforts by *Bowie et al.* [2001] and *Strzepek et al.* [2005]. Recently, there has been an increase in the availability of iron quotas for a range of components of pelagic food webs using techniques such Synchrotron X-ray Fluorescence

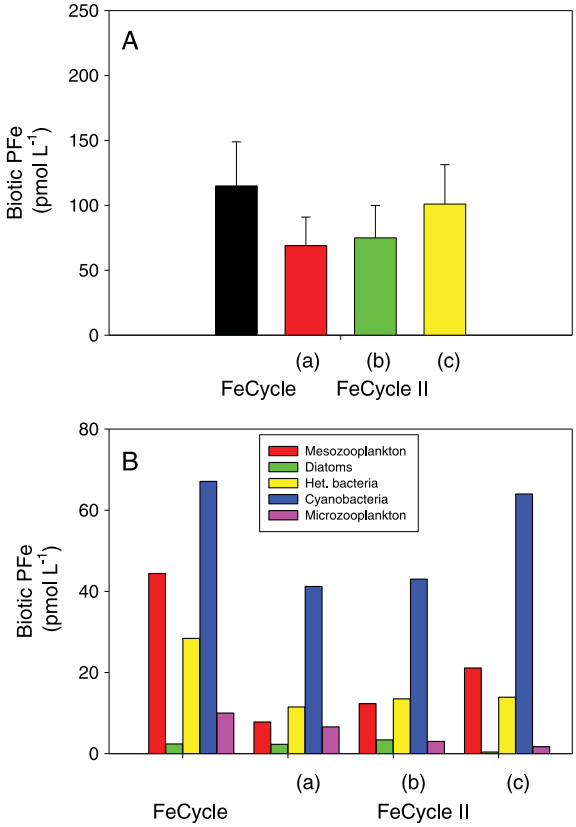

Figure 1. (A) Total column-averaged mixed-layer biotic iron (with error estimates for biotic iron) derived from the Fe quotas presented in Table 3. Biotic iron for FeCycle under steady state conditions and for the distinct bloom phases of FeCycle II: (a) onset (year-day 262), (b) development (year-day 265), and (c) decline (year-day 271) under nonsteady state conditions. For simplicity, error estimates are only provided for the total biotic iron pools but are generally <30% for each taxon [*Twining and Baines*, 2013]. (B) Partitioning of mixed-layer averaged biotic iron during FeCycle under steady state conditions and distinct bloom phases of FeCycle II: (a) onset (year-day 262), (b) development (year-day 265), and (c) decline (year-day 271) under nonsteady state conditions. Pools are expressed as pmol L^{-1} to remove the effect of different mixed-layer depths at each site (for column integrals, see Figure 2). The contribution of autotrophic nanoflagellates to biotic iron was negligible at both sites (Table 1).

(SXRF) [see review in *Twining and Baines*, 2013]; some of which are also presented in Table 3 for the FeCycle II study.

The magnitude of pools of biotic iron is computed as illustrated in the study of *Strzepek et al.* [2005]: the abundance of heterotrophic bacteria ($2.3 \times 10^6 \pm 3.3 \times 10^5$ mL^{-1}) is converted to carbon using a published algorithm giving 3.8 ± 0.6 μmol C L^{-1}; this carbon is then converted to biotic iron (28.4 pmol L^{-1}) using a published Fe:C ratio (7.5 μmol:mol; see Tables 2 and 3). In some cases, the estimates of the error on the measure of biotic Fe are reported [*Sarthou et al.*, 2008], whereas in others, they are not [*Bowie et al.*, 2001; *Strzepek et al.*, 2005]. In the present study, we have retrospectively estimated the error on the biotic iron pools (where not provided) based on a synthesis in *Twining and Baines* [2013, Figure 3] in which they report the standard error of the mean for iron quotas across different regions and taxa. The standard error of the iron quota ranges from <10% to ~30% of the mean in this summary figure. We have used the upper bound of 30% of the mean in all of the error estimates for which error estimates are not published.

The magnitude of the upper ocean biotic iron pool is set primarily by the fluxes of new and recycled iron. The relative contribution of new versus regenerated iron to biological iron uptake is described by the *fe* ratio [biological uptake of new iron / (uptake of new + regenerated iron)] [*Boyd et al.*, 2005]. This ratio is analogous to the classical f-ratio for nitrogen [see *Ward et al.*, 2011]. The *fe* ratio is computed by comparing measured heterotrophic and autotrophic iron uptake (using the ^{55}Fe radio-isotope) versus measured iron recycling [by viral lysis (burst size and microscopy), bacterivory (prey-labelling with ^{55}Fe), and micro- and mesozooplankton herbivory (prey-labelling with ^{55}Fe and SXRF measurements)] as detailed in *Boyd et al.* [2005] and *Boyd et al.* [2012].

3. Results

3.1. Magnitude, Partitioning, and Fate of Biotic Iron Pools

The column-averaged, mixed-layer biotic iron pool concentration during FeCycle, based on published biovolume and iron quotas (Tables 2 and 3), was 118 ± 35 pmol L^{-1} (Figure 1A). It was comparable to that computed using identical published biovolume and iron quotas (with the exception of diatoms, see Table 3), during the onset (69 ± 26 pmol L^{-1}), development (74 ± 32 pmol L^{-1}), and decline (101 ± 49 pmol L^{-1}) phases of the FeCycle II diatom bloom (Figure 1A). Mixed-layer depths during FeCycle ranged from 35 to 50 m [*Croot et al.*, 2007] over 12 days and were ~55, 50, and 30 m for days 262, 265, and 271 during FeCycle II, respectively [*Boyd et al.*, 2012]. Hence, the biotic iron pools were also comparable when expressed as

Table 2. Summary of the Biovolume to Carbon (C) Conversion Factors Used to Compute Biotic C Pools During FeCycle, FeCycle II, SOIREE, and KEOPS, Prior to Estimating Biotic Fe Using the Quotas in Table 3[a]

Study	FeCycle Biovolume:C Algorithm	FeCycle II	SOIREE	KEOPS
Heterotrophic bacteria	12.4 fg C cell^{-1}[b]	12.4 fg C cell^{-1}[b]	20.0 fg C cell^{-1}[h]	12.4 fg C cell^{-1}[b]
Cyanobacteria	250 fg C cell^{-1}[c]	250 fg C cell^{-1}[c]	na	na
Autotrophic flagellates	0.24 pg C μm^{-3}[d]	0.24 pg C μm^{-3}[d]	0.24 pg C μm^{-3}[d]	0.22 pg C um^{-3}[m]
Diatoms/eukaryotic phytoplankton	0.22 pg C μm^{-3}[e]	0.22 pg C μm^{-3}[e]	Size-fractionated chlorophyll and measured C:Chla ratio[i]	Small <85 pg C cell^{-1}; medium 85–488 pg C cell^{-1}; large >488 pg C cell^{-1}[n]
Other phytoplankton groups	na	na	Eukaryotic picophytoplankton 920 fg C cell^{-1}[j]	na
Microzooplankton	0.19 pg C μm^{-3}[f]	0.19 pg C μm^{-3}[f]	0.24 pg C μm^{-3}[k]	0.19 pg C μm^{-3}[f]
Mesozooplankton	C = 40% DW[g]	C = 40% DW[g]	C = 47% DW for copepods[l]	Assumed C = 50% of DW[o]

[a] na = not applicable or not measured; DW = dry weight.
[b] After *Fukuda et al.* [1998], reported in *Strzepek et al.* [2005].
[c] After *Li et al.* [1992], reported in *Strzepek et al.* [2005].
[d] After *Verity et al.* [1992], reported in *Strzepek et al.* [2005].
[e] After *Booth* [1988], reported in *Strzepek et al.* [2005].
[f] After *Putt and Stoecker* [1989], reported in *Strzepek et al.* [2005].
[g] From *Chase and Price* [1997, Table 4], reported in *Strzepek et al.* [2005].
[h] After *Lee and Fuhrman* [1987], reported in *Bowie et al.* [2001, Table 5].
[i] Data obtained during SOIREE, reported in *Bowie et al.* [2001, Table 5].
[j] After *Booth* [1988], reported in *Bowie et al.* [2001, Table 5].
[k] After *Verity et al.* [1992], reported in *Bowie et al.* [2001, Table 5].
[l] After *Davis and Wiebe* [1987], reported in *Zeldis* [2001].
[m] After *Børsheim and Bratbak* [1987], reported in *Christaki et al.* [2008].
[n] After *Cornet-Barthaux et al.* [2007], reported in *Sarthou et al.* [2008].
[o] Reported in *Carlotti et al.* [2008].

Table 3. Summary of the Iron (Fe) Quotas Used to Compute Biotic Fe Pools During FeCycle (Figure 1), FeCycle II (Figure 1), SOIREE (Figure 3), and KEOPS (Figure 3)[a]

Study	FeCycle Fe:C Ratio (μmol:mol)	FeCycle II	SOIREE	KEOPS
Heterotrophic bacteria	7.5[b]	7.5[b]	7.5[b]	7.5[b]
Cyanobacteria	19.0[c]	19.0[c] (17.0)	na	na
Autotrophic flagellates	8.0[d]	8.0[d] (21.0)	7.0[j]	8.0[d]
Diatoms/eukaryotic phytoplankton	2.0[e]	6.0[g] (34.0 *Asterionellopsis*; 16.0, other diatoms)	3.0[k]	4.4[l]
Other phytoplankton groups	na	na	Eukaryotic picophytoplankton 3.0[j]	na
Microzooplankton	11.6[f]	11.6[f]	12.0[f]	11.6[f]
Mesozooplankton	8.0[g]	8.0[g] (30.6[i])	8.0[g]	8.0[g]

[a] For FeCycle II biotic Fe pools presented in Figure 5, direct measurements were used; values in parentheses are from direct measurements from SXRF presented in *King et al.* [2012], with the exception of the mesozooplankton quota, which was obtained from Inductively Coupled Plasma Mass Spectrometry (ICPMS) analysis. na = not applicable as prokaryotic cyanobacteria have not been reported south of the Polar Front.
[b] From *Tortell et al.* [1999], in *Strzepek et al.* [2005, Table 2] and in *Bowie et al.* [2001, Table 5].
[c] From *Brand* [1991], in *Strzepek et al.* [2005, Table 2].
[d] From *Twining et al.* [2004] and *Maranger et al.* [1998], in *Strzepek et al.* [2005, Table 2].
[e] From four species of Southern Ocean diatoms, in *Strzepek et al.* [2005, Table 2].
[f] From *Chase and Price* [1997] and *Twining et al.* [2004], in *Strzepek et al.* [2005, Table 2].
[g] From *Chase and Price* [1997, Table 4] and from *Bowie et al.* [2001, Table 5].
[h] From *Twining et al.* [2004] and *Twining et al.* [2010] (for Southern Ocean diatoms).
[i] From Fe:P ratio of 3.2 mmol:mol for mixed-layer calanoid copepods during FeCycle II using ICPMS converted to Fe:C using a Redfield C:P ratio of 106. Application of the Fe:C ratio of 8.0 used in the other budgets would reduce mesozooplankton iron from 24, 43, and 77 pmol L^{-1} to 6.2, 10.2, and 19.0 pmol L^{-1}.
[j] From *Maranger et al.* [1998] based on the lowest bound for the Fe quotas (iron limited).
[k] Direct measurements during SOIREE, from *Bowie et al.* [2001, Table 5].
[l] From *Sarthou et al.* [2008, Table 5]; ratios are from direct field measurements or lab cultures. In the case of microzooplankton, *Sarthou et al.* had biomass estimates for both heterotrophic ciliates and nanoflagellates, and used the 11.6 quota [*Chase and Price*, 1997] for each of them to estimate biotic iron.

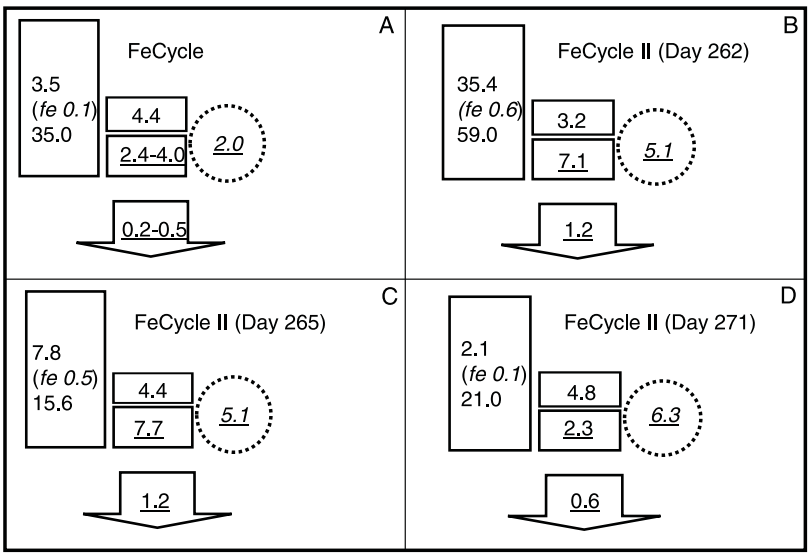

Figure 2. Mixed-layer budgets [column integrals, μmol Fe m^{-2} (pools) and μmol m^{-2} d^{-1} (fluxes, underlined)] in (A) low (FeCycle) and (B–D) high (FeCycle II) iron sites. Days 262, 265, and 271 are budgets from the bloom onset, development, and decline phases, respectively. In each budget, the left-hand box presents the inventory of (top) new iron, (center) the *fe* ratio, and (bottom) the total iron "inventory" equivalent to the new iron inventory multiplied by 1/*fe* ratio. The middle boxes represent the (top) biotic iron pool and (bottom) biological iron uptake [from *Boyd et al.*, 2005, 2012]. The dashed circle denotes rates of iron recycling [from *Boyd et al.*, 2005, 2012], and the downward arrow represents the magnitude of the downward biotic iron flux out of the surface ocean (i.e., intercepted by a surface-tethered free-drifting sediment trap deployed at 100 m depth), respectively. Italics denote recycled iron.

mixed-layer integrals (Figure 2). Thus, the influence of a tenfold larger initial DFe mixed-layer inventory at FeCycle II relative to FeCycle was not reflected in the magnitude of the biotic iron pools.

The reasons for the apparent uniformity in the magnitude of biotic iron pools between sites can be explored further by jointly considering the partitioning of iron across the resident biota (Figure 1B and Table 1), the role of recycling, and the fate of biotic iron in each component of the food web (Figure 2). The biotic iron pool at the FeCycle site was dominated by <2 μm cells (heterotrophic and autotrophic bacteria), with the meso- and microzooplankton also making a significant contribution (Figure 1B). In contrast, the larger phytoplankton, including diatoms and dinoflagellates, made a ~2% contribution (Figure 1B). Despite a much larger inventory of new iron at the FeCycle II site, relative to FeCycle, the partitioning of biotic iron exhibited similar trends during the bloom evolution (Figure 1B). Cells <2 μm dominated the biotic pools, and meso- and microzooplankton also made major contributions to total biotic iron stocks (Figure 1B). Although diatoms dominated the bloom [for example, net primary production; see *Boyd et al.*, 2012], they made a relatively minor contribution (i.e., ~6%) to biotic iron pools during the bloom evolution. Their contribution decreased to even lower levels during the bloom decline, when the biotic iron associated with cyanobacteria and mesozooplankton increased (Figure 1B).

The intercomparison in Figure 1 relied heavily upon the same published iron quotas for each pelagic group (Table 3), and the same groups—mesozooplankton, heterotrophic bacteria, and prokaryotic cyanobacteria—were the dominant contributors to biotic iron pools at both sites, suggesting that the use of the same Fe quotas for each taxon explains the uniformity in biotic iron pools. This suggestion is tested directly later in the text by using direct measurements of Fe quotas for diatoms, cyanobacteria, autotrophic flagellates, and mesozooplankton from FeCycle II (Table 3).

3.2. Differing Fate of Biotic Iron Across the Food Web

Site-specific differences in the relative contribution of recycled iron to the requirements of the resident biota probably offset and compensate for the tenfold differences in the inventories of new iron (Figure 2). Low-iron waters have a *fe* ratio of ~0.1, whereas high-iron waters have higher ratios (Figure 2). Thus, during FeCycle the

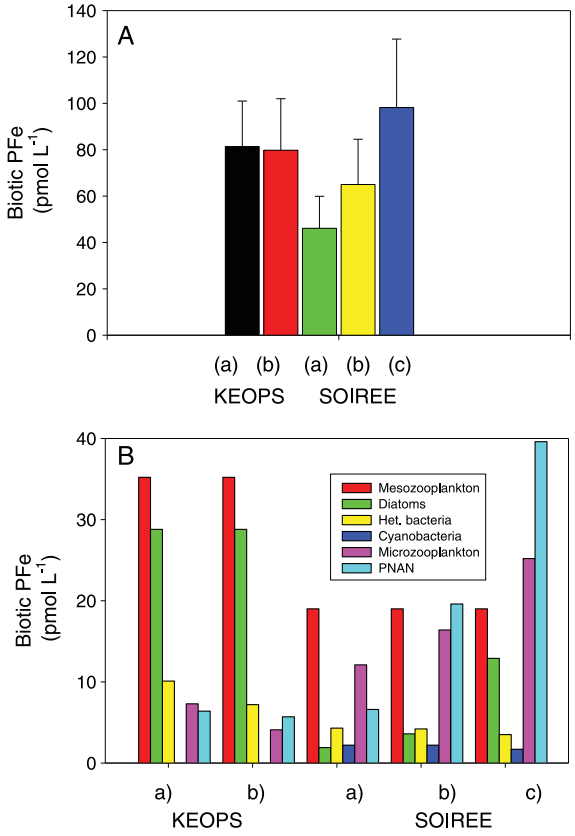

Figure 3. (A) Total column-averaged mixed-layer biotic iron (with error estimates for biotic iron) derived from the Fe quotas presented in Table 3. Biotic iron for the KEOPS natural iron study: (a) the peak of the diatom bloom (year-day 19) and (b) the initial decline of the bloom (year-day 43), and the SOIREE in situ mesoscale iron enrichment: (a) the iron-enriched IN patch (days 1–3) which due to the slow biological response times (days) in polar waters is akin to HNLC waters at this site, (b) the IN patch on day 5, and (c) the IN patch on day 12. For simplicity, error estimates are only provided for the total biotic iron pools but are generally <30% for each taxon [*Twining and Baines*, 2013]. (B) Partitioning of pelagic biotic iron during SOIREE and KEOPS (labelled as for Figure 3A; PNAN denote autotrophic flagellates). Both studies were conducted in waters under nonsteady state conditions. Error estimates for KEOPS Fe quotas are as reported in *Sarthou et al.* [2008] and are estimated for SOIREE (see section 2.1). The mixed-layer depths at each site were ~65 (SOIREE) [*Bowie et al.*, 2001] and 45–55 m [*Blain et al.*, 2007]. Cyanobacteria at the SOIREE site were all eukaryotic (Table 1).

fe ratio of ~0.1 indicates that ninefold more recycled iron will be biologically consumed relative to new iron. When scaled to the FeCycle new iron inventory (3.5 μmol m^{-2}), this results in a "recycled inventory" of 31.5 μmol m^{-2} and a total inventory of 35.0 μmol m^{-2} (Figure 2A), which is ~40% less than the corresponding total inventory at the onset of the FeCycle II bloom (59.0 μmol m^{-2}; Figure 2B).

However, while mixed-layer stocks of new iron appear more akin to a static inventory with little day-to-day change in their magnitude [*Croot et al.*, 2007], that from the recycled iron inventory is more dynamic as it is being "heavily trafficked" [*Morel and Price*, 2003; *Nuester et al.*, 2014] and hence shuttled around on timescales of hours [*Poorvin et al.*, 2004; *Strzepek et al.*, 2005]. The timescales of iron recycling are inextricably linked to the turnover times of much of the microbial and planktonic populations, as the main modes of recycling involve grazing and viral lysis [*Boyd et al.*, 2012; *Evans and Brussard*, 2012; *Matteson et al.*, 2012]. Based on the partitioning of biotic iron, much of this total biotic iron pool is associated with these small, rapidly turned over cells and/or their grazers (Figure 1B). These ecological characteristics help to set the partitioning of biotic iron across the food web, as will the specific iron requirements of each planktonic group [*Morel and Price*, 2003; *Boyd et al.*, 2012].

3.3. Turnover Times for Biotic Iron

A comparison of the biotic iron pools and the rates of biological uptake provides insights into the turnover times for biotic iron. During FeCycle, the size of the pool and the daily rates of iron uptake and recycling are comparable and are much larger than the downward export flux of iron. This comparison of the pools and fluxes implies that most of the biotic iron pool has a turnover time of 24 h, with iron being both remobilized and maintained in the mixed layer, whereas the export flux removes relatively little of this remobilized iron (Figure 2A). During FeCycle II, the uptake and recycling flux of iron are again of similar magnitude (days 262 and 265), and the daily rates when combined are several-fold higher than the size of the biotic iron pool. Surprisingly, this implies a turnover time of 12 h or less of this pool (driven by faster rates of grazing and/or lysis presumably), even though a diatom bloom was developing [*Boyd et al.*, 2012]. The particulate iron export flux is ~10–20% of the recycling flux during FeCycle II, similar to that at the FeCycle site, even though both fluxes are considerably greater at the high-iron site on days 262 and 265 (Figure 2).

The enigma of similarities in biotic iron turnover times at a high- versus a low-iron site is explained by trends in the partitioning of the biotic iron pool (Figures 1 and 2). For example, they reveal that the contribution of the diatom bloom to this pool is less than that for picoplanktonic bacteria during bloom evolution and

decline (Figure 1B). The downward export flux during FeCycle II is driven primarily by directly sinking diatoms and mesozooplankton-derived materials (e.g., fecal pellets) [*Boyd et al.*, 2012; *Twining et al.*, 2014]. During FeCycle II, the fecal iron flux and diatom iron uptake are comparable [1–2 μmol m^{-2} d^{-1}, *Boyd et al.*, 2012] to that of the export flux, suggesting that they may represent a direct throughput into biotic particulate iron export flux and thus a distinctly different pathway for iron to that of the ferrous wheel.

3.4. Other Evidence of Uniform Biotic Iron Pools

The uniformity in biotic iron pools at FeCycle and FeCycle II sites is also evident from data sets from two other high-iron sites—KEOPS (in the Indian Ocean sector of the Southern Ocean) and SOIREE (in the Pacific Ocean sector of the Southern Ocean) (Figure 3A, cf. Figure 1A). During the peak and decline of the natural KEOPS bloom, biotic iron was less than at the low-iron FeCycle and high-iron FeCycle II sites even though chlorophyll *a* concentrations were ~twofold higher than observed at FeCycle II [3 μg (KEOPS) vs. 1.5 μg chlorophyll *a* L^{-1} (FeCycle II) from satellite] [*Blain et al.*, 2007; *Boyd et al.*, 2012]. Estimates for the biotic iron pools were also available for the SOIREE in situ mesoscale iron-enrichment experiment [*Bowie et al.*, 2001]. Again, during SOIREE, despite a diatom-dominated bloom (~1.5 chlorophyll *a* μg L^{-1}), biotic iron pools were similar in magnitude to those during FeCycle and FeCycle II.

In contrast to the FeCycle and FeCycle II sites which were characterized by a similar partitioning in biotic iron across the food web (Figure 1B), the partitioning of biotic iron differed significantly both between the KEOPS and SOIREE sites (Figure 3B and Table 1) and between these polar sites and the FeCycle/FeCycle locales (Figure 3B, cf. Figure 1B and Table 1). Hence, the uniformity in total biotic iron cannot be ascribed (solely) to the use of the same Fe quotas for each taxa present at the sites. Mesozooplankton dominated the KEOPS biotic iron stocks, followed by diatoms and heterotrophic bacteria, whereas autotrophic flagellates, microzooplankton, and mesozooplankton dominated at the SOIREE site (Figure 3B). At both polar sites the contribution of cyanobacteria (mainly eukaryotic; Table 1) to total biotic iron pools was minor.

At KEOPS, diatom iron was around fivefold higher than that for the FeCycle II bloom (Figure 1B, cf. Figure 3B) even though the taxon-specific Fe quota for the latter site was higher than employed in KEOPS (Table 3). As for FeCycle II, at SOIREE, the contributions by diatoms were low, comprising 5–10% of the biotic iron pools despite being the dominant bloom-forming group. The only locale with a considerably lower biotic Fe pool was at the HNLC low-iron "OUT" station during SOIREE (46 ± 14 pmol L^{-1}, i.e., less than half of that during FeCycle; Figures 1A and 3A). As for KEOPS, the SOIREE site was too far south for prokaryotic cyanobacteria to proliferate, with the HNLC assemblage dominated by pico-eukaryotes (with a sixfold lower iron quota compared with pico-prokaryotes; Table 3) and autotrophic nanoflagellates [*Hall and Safi*, 2001]. As prokaryotic cyanobacteria made up >50% of the biotic iron pool during FeCycle (Figure 1B), their absence in polar waters could largely explain the low biotic iron pool at the SOIREE and KEOPS sites and may be a generic feature of HNLC polar waters.

The SOIREE experiment provides the most robust (internally consistent measurement protocols and ecosystem components) comparison of low- versus high-iron waters for biotic C stocks in the mixed layer. At the onset of SOIREE, there was 5.4 μmol C L^{-1} increasing to 9.0 μmol C L^{-1} after 4–5 days of iron enrichment and then 15.8 μmol C L^{-1} by day 12 [*Bakker et al.*, 2006]. So, a ~threefold increase in biotic C stocks, associated with the development of an iron-mediated diatom bloom, took place, but this was not reflected by a comparable increase in biotic iron (Figure 3A). This decoupling between biotic C and Fe is probably due to the increase in the stocks of diatoms, which can have relatively lower iron quotas [*Twining et al.*, 2004; *Strzepek et al.*, 2011, 2012].

3.5. Biotic Iron—Links to Detrital and Lithogenic Fe

In this study, for simplicity, we have focussed on the magnitude of biotic iron pools, even though other iron pools such as detrital and lithogenic are important interlinked components of the iron biogeochemical cycle [*Strzepek et al.*, 2005; *Boyd and Ellwood*, 2010; *King et al.*, 2012]. Both the biotic and detrital iron pools will be influenced by the lithogenic iron pool via photochemically and/or biologically mediated [*Boyd and Ellwood*, 2010] transformations of lithogenic iron to biologically available forms of iron. However, there are presently no direct estimates of the magnitude of the detrital iron pool for the upper ocean [*King et al.*, 2012], with estimates [all obtained by difference, particulate iron minus (lithogenic + biotic)] ranging from >50% to <10% for the HNLC NE subarctic Pacific [*Price and Morel*, 1998] to ~5% for the HNLC subantarctic Pacific

(FeCycle site; [*Frew et al.*, 2006]). Estimates of the contribution of lithogenic iron to the particulate pool (using assumptions regarding the Fe:Al ratio) also reveal a wide range of estimates from 30% [NE subarctic Pacific, 50°N 145°W; *Price and Morel*, 1998] to ~80% [FeCycle site; *Frew et al.*, 2006]. Hence, there is presently insufficient knowledge about the interplay of these pools to expand the present study beyond that of biotic pools.

4. Discussion

4.1. Why Are Biotic Iron Pools Across Different Ocean Domains Uniform?

The examination of the five sites offers a range of potential reasons, both individual and joint, why biotic pools are uniform regardless of DFe concentrations/inventories. They include the following: the application of similar taxon-specific iron quotas (Table 3) in conjunction with comparable pelagic foodweb structures (FeCycle and FeCycle II; Figure 1B); the combined outcome of different pelagic foodweb structures and the wide range of iron quotas for diverse pelagic groups (KEOPS vs. SOIREE; KEOPS vs. FeCycle; Figure 3B, cf. Figure 1B); the linkages between biological turnover times and sources of new versus recycled iron (FeCycle and FeCycle II; Figure 2); and, from the literature, enhanced affinities for transport (e.g., siderophores vs. reductases) in low-iron waters, relative to high-iron waters, result in comparable quotas [*Reuter and Unsworth*, 1991].

4.2. Is Uniformity Due to Using Laboratory Culture Fe:C Ratios?

At each of the five sites considered in the current study, the estimates of biotic iron pools have had to rely almost exclusively on laboratory-based iron quotas (Table 3) due to the prior difficulty in obtaining taxon-specific data in the field. In addition to there being a wide range of iron quotas reported for different pelagic groups, each quota can also vary depending upon environmental conditions such as iron supply [*Chen et al.*, 2011; *Twining and Baines*, 2013]. The flexibility of taxon-specific quotas ranges from threefold [*Kudo and Harrison*, 1997] to ~tenfold [*Brand*, 1991; *Chase and Price*, 1997]. The range of quotas for lab-cultured diatom monocultures may be as high as ~140-fold [*Sunda and Huntsman*, 1995]. The wide range of quotas has been attributed to both environmental controls such as iron nutritional status [*Kudo and Harrison*, 1997], irradiance, and N source [*Maldonado and Price*, 1996; *Strzepek and Harrison*, 2004], and/or to regional oceanic characteristics of the locations from which the species/strains were isolated [*Brand*, 1991]. Such variability was not reflected in the limited number of biovolume/carbon algorithms and iron quotas that could be applied at each of the five sites we examined (Table 3) and hence may explain the uniformity in the biotic iron quotas.

Even an order of magnitude of plasticity in iron quotas could potentially result in large differences in calculated biotic iron pools between sites; however, the application of laboratory culture-derived iron quotas to natural assemblages needs to be put into an environmental context. For example, many of the cyanobacterial isolates used by *Brand* [1991] were not from HNLC waters, and the wide range of quotas reported was based on four orders of magnitude changes in culture medium total dissolved iron concentrations (compared with a tenfold change in dissolved iron from the low- to high-iron field sites in the present study; see Table 4).

Other fundamental differences between the lab-culture experiments and the communities in the field are the forms of iron supplied to laboratory cultures; for example, Fe is usually bound to Ethylenediaminetetraacetic acid (EDTA), an artificial chelator with a binding strength for iron that is many orders of magnitude lower than that of natural high affinity ligands present in seawater. In addition, lab cultures lack the many different forms of iron present in natural seawater, each with a different bioavailability—for example, recycled versus new iron—to different taxa [*Strzepek et al.*, 2005] (Table 4). Taxa differ in their affinity for iron [*Boyd et al.*, 2012], and studies further indicate that the bioavailability of recycled iron can vary between taxa [*Sato et al.*, 2007; *Nuester et al.*, 2014] (Table 4). Taxa that dominate low-iron regions, such as *Synechococcus*, have also been shown to make more efficient use of available iron under such HNLC conditions [*Reuter and Unsworth*, 1991]. Thus, although lab cultures provide robust data for individual species under highly controlled environmental conditions, it is problematic to ascribe quotas from representative "high-iron" or "low-iron" species to specific taxa during field studies. Thus, there is little value in carrying out a sensitivity analysis of how different lab-derived (across the wide range of Fe concentrations employed; Table S1), taxon-specific iron quotas would alter biotic iron pools at oceanic sites (see later).

Table 4. A Summary of Conditions Under Which Lab Culture and Field Studies Were Employed That Provided Estimates of Phytoplankton Iron Quotas[a]

Environmental Properties	Lab Cultures (e.g., Semicontinuous)	Field Studies
Forms of iron	Few	Many—e.g., new vs. regenerated
Dissolved iron (nmol)	1–100	0.2 to ~1
Complexation	EDTA usually	A wide range of ligands (including relatively weakly binding weak L2 and the stronger L1 ligand classes)
Constancy of environment (temperature, irradiance, etc.)	Often steady state*	Nonsteady state (blooms) to quasi steady state (HNLC waters)
Competition	Monoculture	Many phytoplankton species plus microbes
Other environmental factors	Steady state conditions, with some differences in the selected light conditions, and spectral quality	Fluctuating light, nutrient supply, etc. over timescales of hours and days, respectively

[a]A detailed intercomparison across the literature is presented in Table S1 (along with a reference list). Note, from our literature compilation (Table S1), there is a paucity of lab studies of iron limitation that have employed a "continuous" culturing technique (i.e., chemostat or turbidostat), with the majority of iron quota measurements being provided by quasi steady state trace metal-buffered experiments (semicontinuous batch cultures, denoted by *).

In an attempt to minimize this reliance on laboratory-derived Fe quota estimates, during FeCycle II, direct estimates of iron quotas were obtained for *Synechococcus*, autotrophic flagellates, diatoms, and mesozooplankton (Table 3). These revealed up to a threefold range in quotas across diatom species and a lesser range of quotas for autotrophic flagellates (Figure 4A). The observed ranges are comparable for estimates available from other oceanic regions [*Twining et al.*, 2004, 2010]. For example *Synechococcus* also have relatively high Fe quotas in subtropical waters off Bermuda [*Twining et al.*, 2010] that are similar to those reported by *King et al.* [2012] for FeCycle II, suggesting similarities between iron quotas for the same algal groups (potentially driven by their physiological iron requirements) across a range of oceanic regions. Moreover, *King et al.* [2012] averaged these data, across all available phytoplankton groups, to provide an estimate of time-varying iron quotas within the FeCycle II quasi-Lagrangian framework (Figure 4B). As for the individual species, they reveal a small range of Fe quotas (relative to lab culture studies; Table S1) during the bloom evolution.

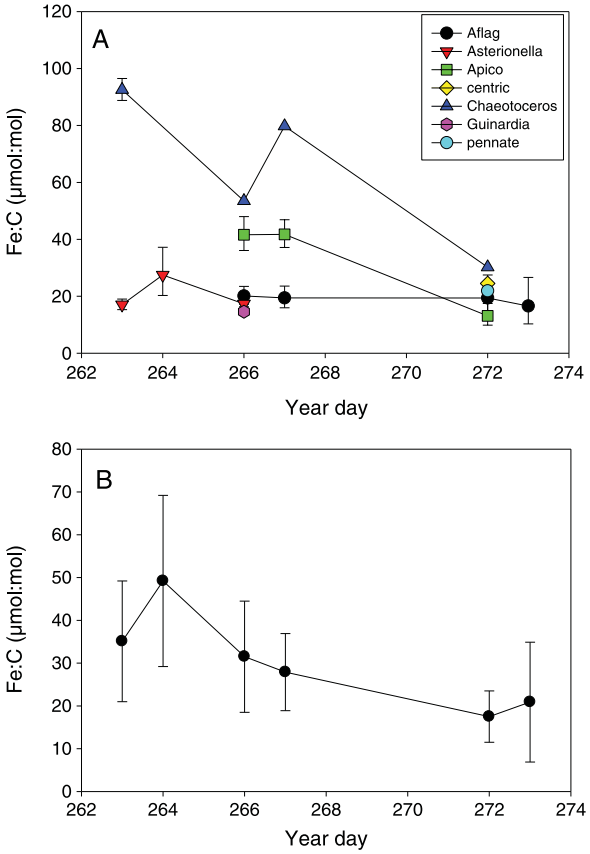

Figure 4. Iron quotas measured in the open ocean during the quasi-Lagrangian FeCycle II experiment for (A) a range of phytoplankton groups using SXRF and (B) the average of these phytoplankton groups [data taken from *King et al.*, 2012, Table 4]. The Fe/P data were converted to Fe/C using the global mean C/P of 133 measured for particulate matter reported in *King et al.* [2012].

Recalculation of biotic iron pools by replacing the published quotas with these direct estimates (mesozooplankton, prokaryotic cyanobacteria, and diatoms) from high-iron, open ocean waters does not result in a significant change in the magnitude of total biotic iron for FeCycle II (Figure 5A, cf. Figure 1A). For FeCycle, we re-estimated total biotic iron by replacing the lab-culture quota for cyanobacteria [from *Brand*, 1991] with the observed value from FeCycle II (and comparable to that reported off Bermuda) and observed

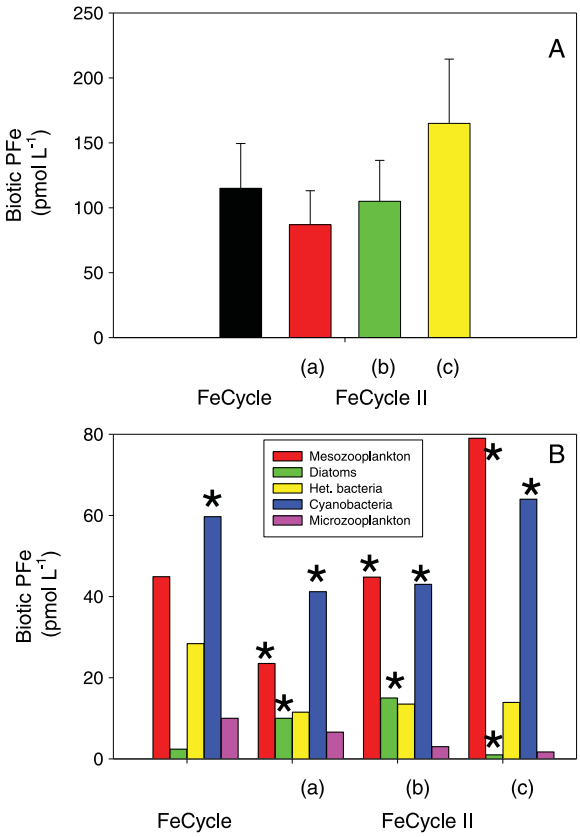

Figure 5. (A) Total column-averaged mixed-layer biotic iron (plus error estimates for the pools) during FeCycle [as presented in Figure 1 but using observed cyanobacterial quotas from FeCycle II], contrasted with those for FeCycle II from direct measurements of iron quotas for mesozooplankton, diatoms, and prokaryotic cyanobacteria (see Table 3), combined with published quotas for heterotrophic bacteria and microzooplankton. (B) Partitioning of mixed-layer biotic iron during FeCycle (as presented in Figure 1 except for the cyanobacteria; derived from direct measurement during FeCycle II denoted by * above the bar graph), and distinct bloom phases of FeCycle II: (a–c) derived from either direct measurements (denoted by * above the bar graphs) or published quotas.

little change in the total biotic iron pool (Figure 5A, cf. Figure 1A). Moreover, the main trends for the components of the pelagic food webs at the FeCycle and FeCycle II sites remained largely unchanged when we used observed quotas as opposed to data from the literature (Table 3). For example, even though a diatom bloom took place during FeCycle II, diatoms were a relatively small proportion of the iron pool (Figure 5B vs. Figure 1B). Also, the mesozooplankton and cyanobacteria were major contributors to the biotic iron pools in FeCycle and FeCycle II (using published Fe quotas; Figure 1B), and this is still the case when employing observed values (Figure 5B). Hence, additional environmental factors, over and above the potential artifactual uniformity introduced by using similar lab-based iron quotas, are probably influencing natural biotic iron pools in the field.

4.3. Is There a Causal Relationship Between *fe* Ratios and Quotas?

The fivefold range in *fe* ratios observed between low- and high-iron surface waters may also play a role in the apparent uniformity of biotic iron pools (Figure 6A). Such differences in iron recycling efficiency (as captured by the *fe* ratio term) likely subsidize biological iron requirements and hence act to buffer and equalize biotic iron pools. Thus, regions characterized by low *fe* ratios offset the limitations imposed by low inventories of new iron, especially for cells that appear to have the highest iron quotas (cyano- and heterotrophic bacteria) since rapid recycling remobilizes the iron needed by these cells (i.e., for every 0.1 nmol L^{-1} of new iron supplied, the low *fe* ratio system remobilizes 0.9 nmol L^{-1}). In contrast, in high-iron, high *fe* ratio systems, substantially more new iron is taken up and proportionately exported from the mixed layer [*Twining et al.*, 2014], and the degree of recycling is less than in HNLC waters (i.e., for every 0.1 nmol L^{-1} of new iron, the high *fe* ratio system remobilizes 0.1 nmol L^{-1}).

There is also evidence of a relationship between prey size and the mode of recycling—for example, small cells such as bacteria are mainly targeted by small-sized recycling agents including viruses [*Poorvin et al.*, 2011] and bacterivores [for example, ~5 μm heterotrophic flagellates with fast growth rates; *Banse*, 1992] (Figure 6B), whereas larger prey such as diatoms will be grazed mainly by larger microzooplankton and mesozooplankton, with implications for the turnover times of iron in large versus small cells. It is likely that this causal relationship is shaped by the composition (and how it varies with time; see Figure 4) and functioning of the biological community present at low- versus high-iron sites.

There appear to be two distinct strategies: diatoms generally have low iron-use (i.e., Fe:C) requirements (but high iron-use efficiencies) [*Strzepek et al.*, 2011], and as bloom formers, they can escape grazing pressure (Figure 7). Hence, diatoms have the potential to retain iron for longer periods (days) within the cell, often

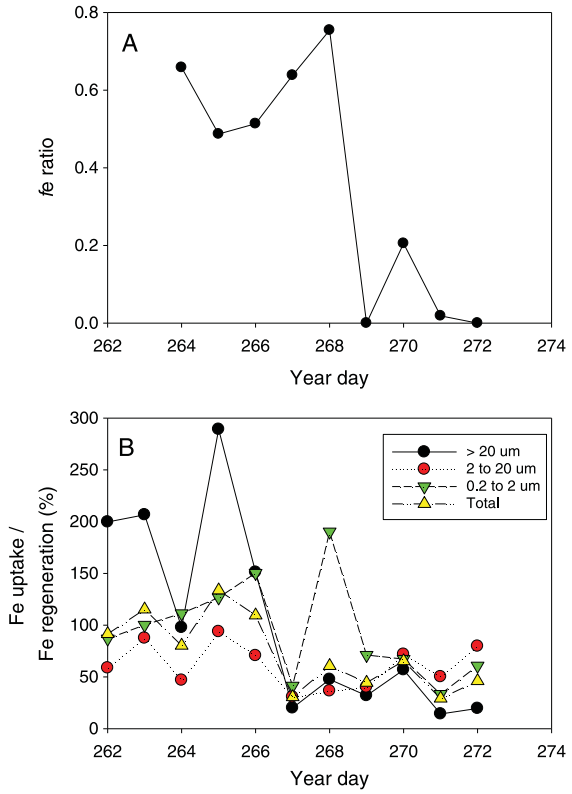

Figure 6. Time series observations during FeCycle II of (A) the *fe* ratio and (B) size-partitioning of iron uptake versus size-dependent iron regeneration processes (0.2–2 μm denotes viral lysis; 2–20 μm includes microzooplankton bacterivory and herbivory; >20 μm targets mesozooplankton grazing). These data were originally reported, in multiple plots, in *Boyd et al.* [2012], and the methods employed are cited there.

being exported directly to depth [*Twining et al.*, 2014], rather than the iron they contain being mobilized through recycling within the ferrous wheel [*Strzepek et al.*, 2005]. In contrast, prokaryotes (cyanobacteria and heterotrophic bacteria) have high affinities for DFe and can accumulate higher biomass-normalized iron quotas, but are prone to rapid recycling via grazing/lysis, and thus, their cellular iron turns over on timescales of hours to days (Figure 7). Prokaryotes use both new iron, when DFe is plentiful [*Boyd et al.*, 2012, Figure 2], and recycled iron that is regenerated and reused rapidly [*Boyd et al.*, 2012]. Based on their larger surface area to volume ratio and generally higher rates of iron uptake, they also outcompete large cells for this scarce resource (Figure 7). Hence, two major biological functional group properties probably make a major contribution to the apparent uniformity of biotic iron pools in regions with different iron status: (1) the ability of prokaryotes to sequester large amounts of iron, which is then retained and remobilized in the ferrous wheel, and (2) the often lower iron requirements of large cells, such as diatoms (see Table 3), along with the high-iron requirements of mesozooplankton.

4.4. Ecological Controls on Iron Quotas in the Ocean?

Unlike in the oceanic nitrogen cycle, where small cells tend to exclusively utilize regenerated nitrogen and larger cells like diatoms take up mainly new nitrogen [*Ward et al.*, 2011], the iron cycle appears to be driven by different rules regarding bioavailability. Both large and small cells, from a range of phytoplankton groups, can take up new iron [*Boyd et al.*, 2012], but it is less clear to what extent large cells can take up regenerated iron, which may have its bioavailability (such as the degree of complexation to strong iron-binding L1 class ligands) altered during recycling [see *Boyd et al.*, 2012, Figure 3]. Hence, iron bioavailability is probably intimately linked with time-varying changes—driven by redox chemistry, biological transformations, and photochemical processing [*Boyd and Ellwood*, 2010]—in dissolved iron inventories, iron quotas, and *fe* ratios over the course of the bloom.

A central challenge to better understanding the controls on taxon-specific iron quotas is to tease apart the temporal effects of changes in dissolved iron concentrations and dissolved iron sources, and shifts in phytoplankton community composition. During FeCycle II, the quotas of individual taxa exhibited a range of temporal signatures, with some groups, for example, autotrophic flagellates (Figure 4A), showing little change, whereas others such as the initially dominant bloom-forming diatom *Asterionellopsis* sp. simply disappeared from the phytoplankton community and provided no information about further temporal shifts in their quotas. The *Chaetoceros*-like diatoms had a ~threefold variation in iron quotas with time and hence with changing dissolved iron concentrations and availability (Figure 6). This latter range of iron quotas is of the same order as those reported for natural phytoplankton communities in response to purposeful iron enrichment in shipboard [*Wilhelm et al.*, 2013] and mesoscale in situ [*Twining et al.*, 2004] studies.

The ranges of iron quotas from open ocean studies are clearly smaller than seen in phytoplankton monocultures (up to 140-fold; Tables 4 and S1) or zooplankton prey-feeding lab studies [up to tenfold;

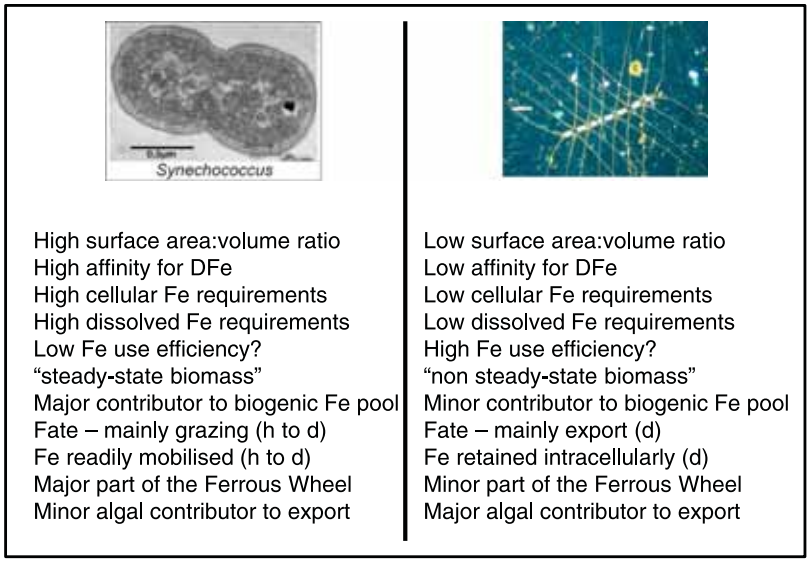

Figure 7. Schematic to contrast the differing roles of (left) prokaryotic cyanobacteria and (right) diatoms in setting the magnitude of biotic pools in low- and high-iron waters. The interplay of species-specific iron quotas, the degree and timescales of retention versus mobilization of biotic iron, and the relative contribution to the ferrous wheel or to biotic iron export are important determinants of biotic iron pools in different oceanic regions. Iron use efficiency is defined here as growth rate × C:Fe molar ratio.

Chase and Price, 1997]. The smaller range of quotas observed in natural communities, relative to laboratory studies, probably reflect that iron availability differs greatly in in vitro (lab-culture studies) relative to in situ (Table 4). For example, in the former the initial pool of dissolved iron typically exceeds (and in many cases greatly exceeds—depending on the chelator used) 4 nmol L^{-1} (Tables 4 and S1), and the use of a trace-metal buffer (e.g., EDTA) ensures that this iron remains more or less constantly available as it is drawn down. In contrast, the dissolved iron pool is <1 nmol L^{-1} (and also there are time-dependent shifts in bioavailability through concurrent changes in the concentration of iron-binding ligands) [*Boyd et al.*, 2012] in most open ocean waters. Thus, over most of the four orders of magnitude range of iron pools in laboratory cultures, the quotas reflect an upper bound of luxury uptake [*Wells et al.*, 1995] and storage.

Another important and influential distinction between the controls on iron quotas in laboratory monocultures and natural settings is the role of inter-specific competition for iron in the latter. It is likely that the lack of competition for resources in laboratory experiments artificially inflates the plasticity in quotas that is reported (Table 4). In contrast, in the open ocean, we propose that once a taxon falls too far below its optimal quota range, it is outcompeted for iron by other groups and is subsequently lost from the community. Such ecological competition demands that at most, organisms can only compete and survive at close to their optimal conditions. Thus, we hypothesize that phytoplankton species have intrinsic "Fe niches." We propose that these niches, along with shifts in the *f*e ratio, will help to set the magnitude of biotic iron pools and reveal how iron biogeochemistry may be influenced by pelagic ecology.

4.5. Ramifications for Ocean Biogeochemistry

The detailed examination of the magnitude and partitioning of biotic iron across oceanic regions (polar, subpolar, and subtropical) characterized by different DFe inventories/concentrations, as presented here, reveals uniformity in the biotic iron pool size and the relative contributions of different planktonic and microbial groups. Even after the consideration of the few available direct measurements of iron quotas (Figure 5), this trend of uniformity, relative to tenfold differences in DFe concentrations/inventories, appears to be valid. More direct measurements of taxon-specific iron quotas are needed to further evaluate the uniformity of biotic iron pools and to assess the potential contribution of the *f*e ratio in setting iron quotas, as these trends may have major ramifications for ocean biogeochemistry [e.g., *Twining et al.*, 2014]. For example, such uniformity hides the very different ecological and biogeochemical traits at

high- versus low-iron sites with respect to carbon biogeochemistry [*Boyd*, 2013], and important processes such as the strength of the biological pump [*Boyd et al.*, 2007; *Blain et al.*, 2007; *Pollard et al.*, 2007]. Furthermore, this uniformity in biotic iron pools across oceanic regions (Figures 1 and 3) suggests that using iron as a modeling currency, as opposed to carbon, may tell us less about how changing conditions will alter ocean biogeochemistry.

Three major issues are evident from this examination of biotic iron pools across five distinct open ocean sites. First, prokaryotic cyanobacteria appear to play a disproportionately important role in setting the magnitude of biotic iron pool in nonpolar waters and in mobilizing iron within the ferrous wheel (Figure 7). In contrast, eukaryotic cyanobacteria play a minor role in biotic iron pool dynamics in polar waters (SOIREE study), due to their sixfold lower iron quotas relative to prokaryotic cyanobacteria (both measured directly; see Table 3).

Second, perhaps the most perplexing issue arising from this study of iron biogeochemistry in five oceanic sites, spanning four oceanic provinces, is why diatoms, characterized by such low-iron pools (Figures 1 and 3), are not more abundant in low-iron HNLC waters. The uniformity of diatom biotic pools across high- and low-iron regions suggests that other factors are restricting their access to iron in HNLC waters, such as being outcompeted by *K* strategists (i.e., smaller phytoplankton with better ability to grow at low dissolved iron concentrations) [*Boyd et al.*, 2012], or differences in iron bioavailability due to cycling by different mechanisms in the ferrous wheel [*Poorvin et al.*, 2004]. It has been proposed that prokaryotes may have the ability to access different pools of iron relative to eukaryotes [*Wilhelm*, 1995], but *Hutchins et al.* [1999] described conditions under which eukaryotes were more capable of accessing specific fractions of the dissolved iron pool. Clearly, the speciation of dissolved iron has the capacity to shape community composition, but there are still very little published data to constrain these relationships.

Another important distinction to consider is that of biological Fe requirements (i.e., Fe:C) and dissolved Fe requirements (i.e., K_m). Diatoms may not need much Fe relative to their biomass, but they may still require higher DFe concentrations to thrive [*Timmermans et al.*, 2004] because of their low surface area to volume quotients limit rates of Fe uptake relative to the Fe needed to support growth. For this reason a bloom-forming phytoplankton group may become Fe limited, even if characterized by relatively low cellular iron requirements.

Third, there is a major disconnect between carbon and iron biogeochemical signatures in low- versus high-iron waters, with carbon budgets revealing more significant differences [*Bakker et al.*, 2006] than for iron. Such pronounced differences in the Fe:C ratios of small versus large cells, with large diatoms fixing threefold more carbon per unit iron during FeCycle II [*Boyd et al.*, 2012] and with carbon content being more strongly linked to cell size than iron content (Table 2), may explain this disjoint between carbon and iron biogeochemistry. Hence, using carbon, rather than iron, in biogeochemical models may more clearly reveal the fundamental physiochemical and biological differences between low- and high-iron waters.

Acknowledgments

M.J.E. research is supported with funding from the Australian Research Council grants (DP0770820, DP110100108, and DP130100679). R.F.S. was supported with funding from the Australian Research Council (DP130100679). BST was supported by grants from the National Science Foundation (OCE-0825379 and OCE-1061545), and D.A.H. was supported by NSF grants OCE-0825319 and ANT-1043748. P.W.B. was supported by New Zealand and Australian Research Council grants. Users can readily access the data from this paper by contacting the corresponding author (Philip.boyd@utas.edu.au), and there are no restrictions on access.

References

Bakker, D. C. E., et al. (2006), Matching carbon pools and fluxes in the Southern Ocean Iron Release Experiment (SOIREE), *Deep Sea Res., Part I*, *53*, 1941–1960, doi:10.1016/j.dsr.2006.08.014.

Banse, K. (1992), Grazing, temporal changes of phytoplankton concentrations, and the microbial loop in the open sea, in *Primary Productivity and Biogeochemical Cycles in the Sea*, edited by P. G. Falkowski and A. D. Woodhead, pp. 409–440, Plenum, New York.

Banse, K. (1996), Low seasonality of low concentrations of surface chlorophyll in the subantarctic water ring: Underwater irradiance, iron, or grazing?, *Prog. Oceanogr.*, *37*, 241–291.

Blain, S., et al. (2007), Effects of natural iron fertilisation on carbon sequestration in the Southern Ocean, *Nature*, *446*, 1070–1074.

Booth, B. C. (1988), Size classes and major taxonomic groups of phytoplankton at two locations in the Subarctic Ocean in May and August, *Mar. Biol.*, *97*, 275–286.

Børsheim, K. Y., and G. Bratbak (1987), Cell volume to cell carbon conversion factors for a bacterivorous *Monas* sp. enriched from sea water, *Mar. Ecol. Prog. Ser.*, *36*, 171–179.

Bowie, A. R., et al. (2001), The fate of added iron during a mesoscale fertilisation experiment in the Southern Ocean, *Deep Sea Res., Part II*, *48*, 2703–2743.

Bowie, A. R., D. Lannuzel, T. A. Remenyi, T. Wagener, P. J. Lam, P. W. Boyd, C. Guieu, A. T. Townsend, and T. W. Trull (2009), Biogeochemical iron budgets of the Southern Ocean south of Australia: Decoupling of iron and nutrient cycles in the subantarctic zone by the summertime supply, *Global Biogeochem. Cycles*, *23*, GB4034, doi:10.1029/2009GB003500.

Boyd, P. W. (2013), Diatom traits regulate Southern Ocean silica leakage, *Proc. Natl. Acad. Sci. U.S.A.*, *110*, 20,358–20,359, doi:10.1073/pnas.1320327110.

Boyd, P. W., and M. J. Ellwood (2010), The biogeochemical cycle of iron in the ocean, *Nat. Geosci.*, *3*(10), 675–682, doi:10.1038/ngeo964.

Boyd, P. W., et al. (2005), FeCycle: Attempting an iron biogeochemical budget from a mesoscale SF6 tracer experiment in unperturbed low iron waters, *Global Biogeochem. Cycles*, *19*, GB4S20, doi:10.1029/2005GB002494.

Boyd, P. W., et al. (2007), Mesoscale iron enrichment experiments 1993–2005: Synthesis and future directions, *Science*, *315*, 612–617.

Boyd, P. W., et al. (2012), Microbial control of diatom bloom dynamics in the open ocean, *Geophys. Res. Lett.*, *39*, L18601, doi:10.1029/2012GL053448.
Brand, L. (1991), Minimum iron requirements of marine-phytoplankton and the implications for the biogeochemical control of new production, *Limnol. Oceanogr.*, *36*, 1756–1771.
Carlotti, F., D. Thibault-Botha, A. Nowaczyk, and D. Lefèvre (2008), Zooplankton community structure, biomass and role in carbon fluxes during the second half of a phytoplankton bloom in the eastern sector of the Kerguelen shelf (January–February 2005), *Deep Sea Res., Part II*, doi:10.1016/j.dsr2.2007.12.010.
Chase, Z., and N. M. Price (1997), Metabolic consequences of iron deficiency in heterotrophic marine protozoa, *Limnol. Oceanogr.*, *42*, 1673–1684.
Chen, X., S. G. Wakeham, and N. S. Fisher (2011), Influence of iron on fatty acid and sterol composition of marine phytoplankton and copepod consumers, *Limnol. Oceanogr.*, *56*(2), 716–724.
Christaki, U., I. Obernosterer, F. Van Wambeke, M. J. W. Veldhuis, N. Garcia, and P. Catala (2008), Microbial food web structure in a naturally iron fertilized area in the Southern Ocean (Kerguelen Plateau), *Deep Sea Res., Part II*, doi:10.1016/j.dsr2.2007.12.009.
Cornet-Barthaux, V., L. Armand, and B. Que´guiner (2007), Biovolume and biomass estimates of key diatoms in the Southern Ocean, *Aquat. Microb. Ecol.*, *48*, 295–308.
Croot, P. L., R. D. Frew, S. Sander, K. A. Hunter, M. J. Ellwood, S. E. Pickmere, E. R. Abraham, C. S. Law, M. J. Smith, and P. W. Boyd (2007), Physical mixing effects on iron biogeochemical cycling: FeCycle experiment, *J. Geophys. Res.*, *112*, C06015, doi:10.1029/2006JC003748.
Davis, C. S., and P. H. Wiebe (1987), Macrozooplankton biomass in a warm core Gulf Stream ring: Time series changes in size structure, taxonomic composition and vertical distribution, *J. Geophys. Res.*, *90*, 8871–8884, doi:10.1029/JC090iC05p08871.
de Baar, H. J. W., L. J. A. Gerringa, P. Laan, and K. R. Timmermans (2008), Efficiency of carbon removal per added iron in ocean iron fertilization, *Mar. Ecol. Prog. Ser.*, *364*, 269–282, doi:10.3354/meps07548.
Ellwood, M. J., S. D. Nodder, A. King, D. A. Hutchins, S. W. Wilhelm, and P. W. Boyd (2014), Pelagic iron cycling during the subtropical spring bloom, east of New Zealand, *Mar. Chem.*, *160*, 18–33.
Evans, C., and C. P. D. Brussard (2012), Viral lysis and microzooplankton grazing of phytoplankton throughout the Southern Ocean, *Limnol. Oceanogr.*, *57*, 1826–1837, doi:10.4319/lo.2012.57.6.1826.
Fasham, M. J. R., P. W. Boyd, and G. Savidge (1999), Modeling the relative contributions of autotrophs and heterotrophs to carbon flow at a Lagrangian JGOFS station in the Northeast Atlantic: The importance of DOC, *Limnol. Oceanogr.*, *44*, 80–94.
Frew, R. D., D. A. Hutchins, S. Nodder, S. Sanudo-Wilhelmy, A. Tovar-Sanchez, K. Leblanc, C. E. Hare, and P. W. Boyd (2006), Particulate iron dynamics during FeCycle in subantarctic waters southeast of New Zealand, *Global Biogeochem. Cycles*, *20*, GB1S93, doi:10.1029/2005GB002558.
Fukuda, R., H. Ogawa, T. Nagata, and I. Koike (1998), Direct determination of carbon and nitrogen contents of natural bacterial assemblages in marine environments, *Appl. Environ. Microbiol.*, *64*, 3352–3358.
Hall, J. A., and K. Safi (2001), The impact of in situ Fe fertilisation on the microbial foodweb in the Southern Ocean, *Deep Sea Res., Part II*, *48*, 2591–2614.
Hutchins, D. A., and K. W. Bruland (1998), Iron-limited diatom growth and Si : N uptake ratios in a coastal upwelling regime, *Nature*, *393*, 561–564, doi:10.1038/31203.
Hutchins, D. A., A. E. Witter, A. Bulter, and G. W. Luther III (1999), Competition among marine phytoplankton for different chelated iron species, *Nature*, *400*, 858–861.
King, A. L., S. A. Sanudo-Wilhelmy, P. W. Boyd, B. S. Twining, S. W. Wilhelm, C. Breene, M. J. Ellwood, and D. A. Hutchins (2012), A comparison of biogenic iron quotas during a diatom spring bloom using multiple approaches, *Biogeosciences*, *9*, 667–687.
Kudo, I., and P. J. Harrison (1997), Effect of iron nutrition on the marine cyanobacterium *Synechococcus* grown on different N sources and irradiances, *J. Phycol.*, *33*, 232–240, doi:10.1111/j.0022-3646.1997.00232.x.
Lee, S., and J. A. Fuhrman (1987), Relationships between biovolume and biomass of naturally derived marine bacterioplankton, *Appl. Environ. Microbiol.*, *53*, 1298–1303.
Li, W. K., P. M. Dickie, B. D. Irwin, and A. M. Wood (1992), Biomass of bacteria, cyanobacteria, prochlorophytes and photosynthetic eukaryotes in the Sargasso Sea, *Deep Sea Res. A*, *39*, 501–519.
Longhurst, A. R. (2007), *Ecological Geography of the Sea*, pp. 527, Academic Press, San Diego.
Maldonado, M. T., and N. M. Price (1996), Influence of N substrate on Fe requirements of marine centric diatoms, *Mar. Ecol. Prog. Ser.*, *141*, 161–172.
Maranger, R., D. F. Bird, and N. M. Price (1998), Iron acquisition by photosynthetic marine phytoplankton from ingested bacteria, *Nature*, *396*, 248–251.
Martin, J. H., R. M. Gordon, S. Fitzwater, and W. W. Broenkow (1989), Vertex: Phytoplankton/iron studies in the Gulf of Alaska, *Deep Sea Res. A*, *36*, 649–680.
Matteson, A. R., S. N. Loar, S. Pickmere, J. M. DeBruyn, M. J. Ellwood, P. W. Boyd, D. A. Hutchins, and S. W. Wilhelm (2012), Production of viruses during a spring phytoplankton bloom in the South Pacific Ocean near of New Zealand, *FEMS Microb. Ecol.*, *79*, 709–719.
Mauchline, J. (1998), *The Biology of Calanoid Copepods*, Advances in Marine Biology, vol. 33, pp. 710, Elsevier Academic Press, San Diego, Calif.
Montagnes, D. J. S., J. A. Berges, P. J. Harrison, and F. J. R. Taylor (1994), Estimating carbon, nitrogen, protein, and chlorophyll a from volume in marine phytoplankton, *Limnol. Oceanogr.*, *39*, 1044–1060.
Moore, C. M., et al. (2009), Large-scale distribution of Atlantic nitrogen fixation controlled by iron availability, *Nat. Geosci.*, *2*, 867–871, doi:10.1038/NGEO667.
Moore, J. K., and S. C. Doney (2007), Iron availability limits the ocean nitrogen inventory stabilizing feedbacks between marine denitrification and nitrogen fixation, *Global Biogeochem. Cycles*, *21*, GB2001, doi:10.1029/2006GB002762.
Moore, J. K., S. C. Doney, and K. Lindsay (2004), Upper ocean ecosystem dynamics and iron cycling in a global 3D model, *Global Biogeochem. Cycles*, *18*, GB4028, doi:10.1029/2004GB002220.
Morel, F. M. M., and N. M. Price (2003), The biogeochemical cycles of trace metals in the oceans, *Science*, *300*, 944–947.
Nuester, J., S. Shema, A. Vermont, D. M. Fields, and B. S. Twining (2014), The regeneration of highly bioavailable iron by meso- and microzooplankton, *Limnol. Oceanogr.*, *59*, 1399–1409.
Pollard, R., R. Sanders, M. Lucas, and P. Statham (2007), The Crozet Natural Iron Bloom and Export Experiment (CROZEX), *Deep Sea Res., Part II*, *54*, 1905–1914.
Poorvin, L., J. M. Rinta-Kanto, D. A. Hutchins, and S. W. Wilhelm (2004), Viral lysis as a major source of bioavailable iron in marine ecosystems, *Limnol. Oceanogr.*, *49*, 1734–1741.
Poorvin, L., S. G. Sander, I. Velasquez, E. Ibisanmi, G. R. LeCleir, and S. W. Wilhelm (2011), Comparative bioavailability and Fe-binding of a catecholate siderophore and virus-mediated lysates from the marine bacterium Vibrio alginolyticus PWH3a, *J. Exp. Mar. Biol. Ecol.*, *399*, 43–47.

Price, N. M., and F. M. M. Morel (1998), Biological cycling of iron in the ocean, in *Iron Transport and Storage in Microorganisms, Plants, and Animals*, Metal Ions in Biological Systems, vol. 35, edited by A. Sigel and H. Sigel, pp. 1–36, M. Dekker Inc., New York.
Putt, M., and D. K. Stoecker (1989), An experimentally determined carbon—Volume ratio for marine oligotrichous ciliates from estuarine and coastal waters, *Limnol. Oceanogr.*, *34*, 1097–1103.
Reuter, J. G., and N. L. Unsworth (1991), Response of marine *Synechococcus* (Cyanophyceae) cultures to iron nutrition, *J. Phycol.*, *27*, 173–178.
Sarthou, G., D. Vincent, U. Christaki, I. Obernosterer, K. R. Timmermans, and C. P. D. Brussaard (2008), The fate of biotic iron during a phytoplankton bloom induced by natural fertilization: Impact of copepod grazing, *Deep Sea Res., Part II*, *55*, 734–751.
Sato, M., S. Takeda, and K. Furuya (2007), Iron regeneration and organic iron(III)-binding ligand production during in situ zooplankton grazing experiment, *Mar. Chem.*, *106*, 471–488, doi:10.1016/j.marchem.2007.05.001.
Strzepek, R. F., and P. J. Harrison (2004), Photosynthetic architecture differs in coastal and oceanic diatoms, *Nature*, *431*, 689–692.
Strzepek, R. F., M. T. Maldonado, J. L. Higgins, J. Hall, K. Safi, S. W. Wilhelm, and P. W. Boyd (2005), Spinning the "Ferrous Wheel": The importance of the microbial community in an iron budget during the FeCycle experiment, *Global Biogeochem. Cycles*, *19*, GB4S26, doi:10.1029/2005GB002490.
Strzepek, R. F., M. T. Maldonado, K. A. Hunter, R. D. Frew, and P. W. Boyd (2011), Adaptive strategies by Southern Ocean phytoplankton to lessen iron limitation: Uptake to organically-complexed iron and reduced cellular iron requirements, *Limnol. Oceanogr.*, *56*, 1983–2002.
Strzepek, R. F., K. A. Hunter, R. D. Frew, P. J. Harrison, and P. W. Boyd (2012), Iron-light interactions differ in Southern Ocean phytoplankton, *Limnol. Oceanogr.*, *57*(4), 1182–1200, doi:10.4319/lo.2012.57.4.1182.
Sunda, W. G., and S. A. Huntsman (1995), Iron uptake and growth limitation in oceanic and coastal phytoplankton, *Mar. Chem.*, *50*, 189–206.
Timmermans, K. R., B. van der Wagt, and H. J. W. deBaar (2004), Growth rates, half-saturation constant, and silicate, nitrate, and phosphate depletion in relation to iron availability of four large, open-ocean diatoms from the Southern Ocean, *Limnol. Oceanogr.*, *49*, 2141–2151.
Tortell, P. D., M. T. Maldonado, J. Granger, and N. M. Price (1999), Marine bacteria and biogeochemical cycling of iron in the oceans, *FEMS Microbiol. Ecol.*, *29*(1), 1–11.
Turner, S. M., M. J. Harvey, C. S. Law, P. D. Nightingale, and P. S. Liss (2004), Iron-induced changes in oceanic sulfur biogeochemistry, *Geophys. Res. Lett.*, *31*, L14307, doi:10.1029/2004GL020296.
Twining, B. S., and S. B. Baines (2013), The trace metal composition of marine phytoplankton, *Annu. Rev. Mar. Sci.*, *5*, 191–215.
Twining, B. S., S. B. Baines, and N. S. Fisher (2004), Element stoichiometries of individual plankton cells collected during the Southern Ocean Iron Experiment (SOFeX), *Limnol. Oceanogr.*, *49*, 2115–2128.
Twining, B. S., D. Nunez-Milland, S. Vogt, R. S. Johnson, and P. N. Sedwick (2010), Variations in *Synechococcus* cell quotas of phosphorus, sulfur, manganese, iron, nickel, and zinc within mesoscale eddies in the Sargasso Sea, *Limnol. Oceanogr.*, *55*, 492–506.
Twining, B. S., S. D. Nodder, A. L. King, D. A. Hutchins, G. R. LeCleir, J. M. DeBruyn, E. W. Maas, S. Vogt, S. W. Wilhelm, and P. W. Boyd (2014), Differential remineralization of major and trace elements in sinking diatoms, *Limnol. Oceanogr.*, *59*(3), 689–704.
Verity, P. G., C. Y. Robertson, C. R. Tronzo, M. G. Andrews, J. R. Nelson, and M. E. Sieracki (1992), Relationships between cell-volume and the carbon and nitrogen content of marine photosynthetic nanoplankton, *Limnol. Oceanogr.*, *37*, 1434–1446.
Ward, B. B., A. P. Rees, P. J. Somerfield, and I. Joint (2011), Linking phytoplankton community composition to seasonal changes in f-ratio, *ISME J.*, *5*, 1759–1770.
Wells, M. L., N. M. Price, and K. W. Bruland (1995), Iron chemistry in seawater and its relationship to phytoplankton: A workshop report, *Mar. Chem.*, *48*, 157–182.
Wilhelm, S. W. (1995), Ecology of iron-limited cyanobacteria: A review of physiological responses and implications for aquatic systems, *Aquat. Microb. Ecol.*, *09*, 295–303, doi:10.3354/ame009295.
Wilhelm, S. W., et al. (2013), Elemental quotas and physiology of a southwestern Pacific Ocean plankton community as a function of iron availability, *Aquat. Microb. Ecol.*, *68*, 185–194.
Zeldis, J. (2001), Mesozooplankton community composition, feeding, and export production during SOIREE, *Deep Sea Res., Part II*, *48*, 2615–2634.